Temperature profile for glacial ice at the South Pole: Implications for life in a nearby subglacial lake

P. Buford Price*†, Oleg V. Nagornov‡, Ryan Bay*, Dmitry Chirkin*, Yudong He§, Predrag Miocinovic*, Austin Richards¶, Kurt Woschnagg*, Bruce Koci‖, and Victor Zagorodnov**

*Physics Department, University of California, Berkeley, CA 94720; ‡Moscow Engineering Physics Institute, Moscow 115409, Russia; §Rosetta Inpharmatics, 12040 115th Avenue, Kirkland, WA 98034-4399; ¶Indigo Systems Corporation, 5385 Hollister Avenue, No. 103, Santa Barbara, CA 93111; ‖Space Sciences and Engineering Laboratory, University of Wisconsin, Madison, WI 53706; and **Byrd Polar Research Center, Ohio State University, Columbus, OH 43210

Contributed by P. Buford Price, April 22, 2002

Airborne radar has detected ≈100 lakes under the Antarctic ice cap, the largest of which is Lake Vostok. International planning is underway to search in Lake Vostok for microbial life that may have evolved in isolation from surface life for millions of years. It is thought, however, that the lakes may be hydraulically interconnected. If so, unsterile drilling would contaminate not just one but many of them. Here we report measurements of temperature vs. depth down to 2,345 m in ice at the South Pole, within 10 km from a subglacial lake seen by airborne radar profiling. We infer a temperature at the 2,810-m deep base of the South Pole ice and at the lake of −9°C, which is 7°C below the pressure-induced melting temperature of freshwater ice. To produce the strong radar signal, the frozen lake must consist of a mix of sediment and ice in a flat bed, formed before permanent Antarctic glaciation. It may, like Siberian and Antarctic permafrost, be rich in microbial life. Because of its hydraulic isolation, proximity to South Pole Station infrastructure, and analog to a Martian polar cap, it is an ideal place to test a sterile drill before risking contamination of Lake Vostok. From the semiempirical expression for strain rate vs. shear stress, we estimate shear vs. depth and show that the IceCube neutrino observatory will be able to map the three-dimensional ice-flow field within a larger volume (0.5 km^3) and at lower temperatures (−20°C to −35°C) than has heretofore been possible.

Measurement of Temperature Profile

Through a chain of observations, measurements at the AMANDA (Antarctic Muon and Neutrino Detector Array) neutrino observatory in deep ice at the South Pole (1) have provided an impetus for exploration for life in subglacial lakes. As essential steps in the analysis of high-energy neutrino data, Woschnagg *et al.* (2) measured optical absorption and scattering coefficients as a function of depth in the glacial ice, and Price *et al.* (3) determined dust concentration and age as a function of depth by using light sources and detectors installed in the ice. To measure temperature as a function of depth, from which the rate of shear of the AMANDA structure could be estimated, the collaboration installed thermistors at depths from 800 m to 2,345 m in boreholes produced with hot-water drilling. We will return to the question of deformation rate later.

The temperatures were measured by Omega Engineering (Stamford, CT) 44031 thermistors. The thermistors were cast into plastic molds and attached to each of 20 AMANDA cables at various locations for a total of 59 measurement points. The cables were deployed at times ranging from the 1993–1994 to the 1999–2000 austral seasons. All thermistors were read out in July 2001 by a Hewlett–Packard-3478 multimeter, after dwell times adequately long (1.5–7.5 yr) for recovery of the refrozen ice to ambient temperature. The measurement uncertainty ranged from 0.24°C for the shallowest depths to 0.11°C for the deepest depths.

The depths of the thermistors were determined by correlating thermistor location on the cable to the closest optical module on the same cable. The AMANDA collaborators used optical methods to measure relative depths of the optical modules, and they calculated the absolute depth of the AMANDA array by combining cable payout with pressure of the water column at the time of deployment for each cable. Estimates of thermistor depths are good to ±2 m.

Fig. 1 shows the data. Included are unpublished measurements of temperature in South Pole ice at depths of 12–50 m by Giovinetto (4).

Extrapolation of Temperature to Bedrock

We now discuss how to use the heat-transfer equation to calculate the temperatures from 2,345 m to bedrock at 2,810 m, based on the data in Fig. 1. For ice located on a dome-shaped glacier the heat-transfer equation would simplify to one (vertical) dimension, and the main subtlety would be the effect of past changes in surface temperature, which propagate downward by thermal diffusion with amplitudes that die out with depth. For a sloped location such as is the case at the South Pole, a precise analysis at all depths would require use of a two-dimensional equation, the second dimension being along the direction of downhill flow of the glacier. However, since our purpose is to find the temperature at the base, we do not have to fit the full temperature profile but only the bottom portion, which is relatively insensitive to changes of surface temperature. For a thick ice sheet such as is the case at South Pole, the temperature distribution near the ice-bedrock interface depends mainly on the geothermal heat flux, which is a parameter of the model; temperature changes near the surface are strongly attenuated at the bottom (5, 6).

Profiles of temperature vs. depth exist for two other locations that are both deep and sloped. Measured and calculated profiles of temperature vs. depth at Camp Century, Greenland, coincide to better than 0.1°C from a depth of 200 m down to bedrock (7). Measured and calculated profiles at Byrd Station, Antarctica, agree to within 0.2°C (5). In both cases the assumption of steady-state ($\theta/\theta t = 0$, with θ = temperature in °C) was found to be applicable. Deviations from a linear dependence in the lowest parts of those glaciers are small despite relatively large slopes and horizontal surface velocities: 0.0037 radian and 5.5–10 m/yr for Camp Century (7) and ≈0.004 radian and 12.8 m/yr for Byrd Station (5).

For the Antarctic continent the BEDMAP consortium has produced a suite of integrated digital topographical models that incorporate all available data (8). We extracted values of surface elevation, bedrock elevation, and ice thickness tabulated at intervals of 5 km × 5 km. The data show that the ice at the South Pole is 2,810 m thick; the ice surface near the Pole has a smooth downward slope α ≈0.0015 radian to the northwest; and the average downward slope at bedrock is ≈0.0015 radian in about the same direction. The bedrock surface contains local hills and holes with maximal deviation of ±100 m in the region within ≈50

Abbreviations: AMANDA, Antarctic Muon and Neutrino Detector Array; kyr, kiloyears.

†To whom reprint requests should be addressed. E-mail: bprice@uclink4.berkeley.edu.

 www.pnas.org/cgi/doi/10.1073/pnas.082238999

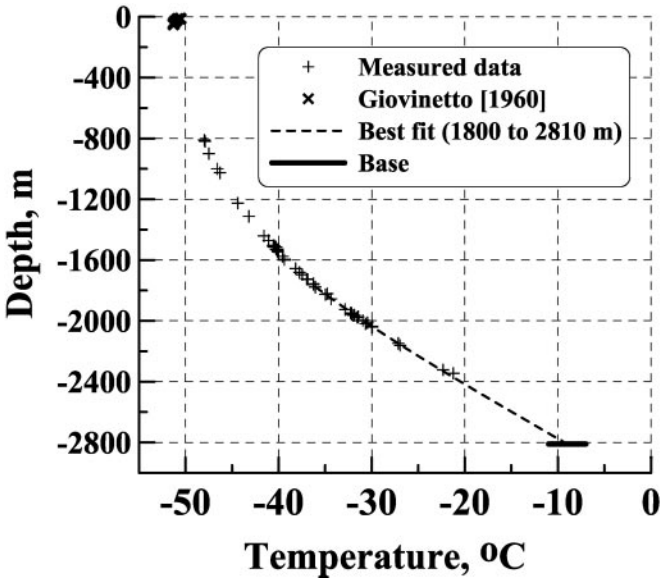

Fig. 1. Temperatures measured in deep AMANDA boreholes (+, this work) and in a shallow borehole [×, Giovinetto (4)], compared with best-fit temperature profile for the deepest 1,000 m. The dashed curve, which gave a basal temperature of −9°C and a geothermal flux of 61 mW/m^2, used vertical advection vs. depth derived from depth vs. age data (3). Two Dansgaard–Johnsen models of vertical advection that bracketed the derived advection curve gave basal temperatures less than 1°C warmer.

km of the Pole. A 1998 airborne radar profile confirms that ice close to the Pole consists of an almost parallel-sided slab with very small slope.[††] Eq. **1** for heat transfer in ice sheets therefore can be written in two-dimensional form (9). It describes ice temperature as a function of time t, with coordinate x and velocity component u directed along the ice-bedrock interface, and z, the vertical coordinate, positive downward from the surface.

$$\rho c\left(\frac{\partial\theta}{\partial t}+u\,\frac{\partial\theta}{\partial x}+w\,\frac{\partial\theta}{\partial z}\right)=\frac{\partial}{\partial x}\left(K\,\frac{\partial\theta}{\partial x}\right)+\frac{\partial}{\partial z}\left(K\,\frac{\partial\theta}{\partial z}\right)+Q, \quad [1]$$

where ρ, c, and K are density, specific heat capacity, and thermal conductivity of ice, respectively; w is the vertical advection rate; and Q is the rate of internal heat generation per unit volume caused by ice shear.

The penetration of seasonal and long-period temperature changes from the surface has been analyzed by Hanson and Dickinson (10). They found that the accumulation rate significantly affects the penetration depth of the temperature signal only for wavelengths that are large compared with the thickness of the glacier. As an example, the amplitude of a 10°C step in temperature at the surface decreases to <0.1°C at 2,000-m depth for periods up to 15 kiloyears (kyr). For depths >2,000 m in which we are interested, the measurements are immune to surface temperature changes on a time scale $\ll$ 15 kyr. The term θ/t in Eq. **1** can thus be neglected for the bottom part of the South Pole ice, which simplifies the calculation of temperatures in the lowest few hundred meters where measurements have not been made.

We can further simplify Eq. **1** by eliminating the terms $\rho c(u\partial\theta/\partial x)$ and $\partial/\partial x(K\partial\theta/\partial x)$. To do that, we first show that $-w\,\partial\theta/\partial z$ (the vertical advection) and Q (responsible for internal heating of the glacier caused by ice shear) have a negligible effect on the temperature distribution in the bottom part of the glacier. The influence of vertical advection on the solution of the steady-state heat transfer equation has been discussed by Paterson (9). For both the Nye model (discussed in ref. 9) and the more physically reasonable Dansgaard–Johnsen model (11), we find that at depths from 2,200 m to bedrock the deviation, caused by vertical advection, of the temperature profile from a straight line is <3% and <1%, respectively, which is within the accuracy of the temperature measurements.

For two reasons, internal heating, Q, is significant only in the bottom part of the glacier. First, the shear stress along the flow direction on a block inclined at angle α increases with the mass of overlying ice, as $\tau_{xz}=\rho gz\cdot\sin\alpha$, where g is gravitational acceleration. The heat dissipation rate is $Q=2\tau_{xz}\cdot d\varepsilon_{xz}/dt$, where $d\varepsilon_{xz}/dt$ is the strain rate given by Glen's semiempirical flow law,

$$d\varepsilon_{xz}/dt=A(\theta)\tau_{xz}^3 \quad [2]$$

with exponent $n\approx3$. Second, $A(\theta)$ increases with temperature as $\exp(-U/kT)$, as a result of which $d\varepsilon_{xz}/dt$ is 2–3 orders of magnitude higher for ice near bedrock than for surface ice, which has a temperature of −51° at the South Pole. $A(\theta)$ also depends on climatic conditions (9), being about 2.5 times larger for pre-Holocene ice than for Holocene ice (9), because of a fabric in pre-Holocene ice that favors deformation in shear. We find that the contribution of a depth-dependent $Q(z)$ in the heat flux at the bed is 2 orders of magnitude less than the geothermal flux from bedrock and can be neglected in Eq. **1**.

The fact that the measured temperatures decrease linearly with depth in the bottom part of the Camp Century and Byrd Station glaciers allows us to conclude that the horizontal components of advection, $\rho c(u\partial\theta/\partial x)$, and thermal diffusion, $\partial/\partial x(K\partial\theta/\partial x)$, are insignificant near the bottom of the glacial ice at South Pole. This is explained as follows. Near the South Pole the glacial ice is very nearly a slab with parallel top and bottom surfaces and with slope of only ≈0.0015 (8). Because of local variations in air temperatures, the surfaces of constant temperature near the upper surface of the ice may not be parallel to each other. However, as we have seen, changes in temperature propagating downward from the surface attenuate exponentially with depth, so that only very long-period climatic variations can penetrate to the glacier bottom, and they do so with small amplitude. As a consequence, thermal diffusion greatly reduces gradients in horizontal directions. Heat can also be transported by horizontal advection. The flow velocity at the ice-bedrock interface and in stagnant zones near rough interfaces is essentially zero. The flow lines in the bottom part of the South Pole ice are practically parallel to the averaged bedrock boundary, and we can thus neglect the terms $\rho c(u\partial\theta/\partial x)$ and $\partial/\partial x(K\partial\theta/\partial x)$ in Eq. **1** because the derivatives are taken along lines of constant temperature that are parallel to the flow lines along x.

Thus, at great depths in the ice the heat-flow equation reduces to the simple one-dimensional steady-state form for purposes of estimating the basal temperature and the geothermal flow in South Pole ice.

$$\rho cw\,\frac{d\theta}{dz}=\frac{d}{dz}\left(K\,\frac{d\theta}{dz}\right)+Q, \quad [3]$$

In solving this equation, we first tried imposing a boundary condition that the temperature at the glacier-bedrock interface be at the pressure-melting point, −2°C. With this constraint the calculated steady-state profile fell far below the observed one. The deviation from measured temperatures was 4°C at depth 2,000 m, growing to 10°C at 1,000 m. To obtain a fit with the lowest measured points we were forced to allow the temperature at the bedrock interface to be below the pressure-melting point.

[††]Blankenship, D. D. and Instrument Definition Team for a Europa Radar Sounder, Lunar and Planetary Conference XXXII, March 12–16, 2001, Houston, abstr. 1854.

Vertical advection is the consequence of snow accumulation at the surface and lateral flow of ice under compression. The average accumulation rate in the last $\approx 10^3$ yr at the South Pole was 0.073 m ice/yr (12). Data for ^{10}Be as a function of depth (13) show that this rate was representative only of warm periods such as the Holocene (0–18 kyr) and the Eemian (118–137 kyr), alternating with glacial periods (18–118 and >137 kyr) for which the accumulation rate was a factor 2–3 smaller. In solving Eq. **3** we tried in turn each of four different assumptions: (*i*) accumulation rate = 0.073 cm/yr; (*ii*) depth-dependent advection rate based on ^{10}Be data (13), scaled to South Pole ice; (*iii*) vertical advection rate vs. depth derived by finding the slope of the depth vs. age curve for South Pole ice (3), which we approximated by $w(z) = w_0(1 - z/H)^m$, with $w_0 = 0.073$ cm/yr and $m = 1.317$; and (*iv*) use of the Dansgaard–Johnsen model (11) for vertical advection, which applies for ice frozen at the base. For *iv*, we took the vertical strain rate to be constant in the upper 75% of the glacier and from there decreasing linearly to zero at the bed. For constant accumulation rates of 3.0 and 7.3 cm/yr, the Dansgaard–Johnsen model gave lower and upper estimates for the measured depth vs. age dependence (3).

We solved Eq. **3** with boundary conditions

$$\theta\Big|_{z=z_1} = \theta_{z_1} \text{ and } -k\frac{\mathrm{d}\theta}{\mathrm{d}z}\Big|_{z=H} = q_B,$$

where θ_{z1} is the temperature at depth z_1 and q_B is the heat flux from bedrock into ice. For fully compacted ice, density depends on pressure p (in Pa) and temperature θ (in °C) as $\rho_\theta = 916.8\cdot[1 + 0.94\cdot10^{-12}(p - 10^5)][1 - 1.53\cdot10^{-4}\theta]$ kg/m^3. Kuivinen *et al.* (14) measured density of South Pole ice in the firn layer and down to 200 m, below which it is fully dense. We fitted their data with the expression $\rho(z,\theta) = (1 - a\cdot\exp(-b\,z))\cdot\rho_\theta$ with $a = 0.61$, $b = 0.0175$. For heat capacity of pure ice we took c (in J/(kg·°C) = 2,115 + 7.79 θ with θ in °C. For thermal conductivity, with T in °K, we used $K = 9.828\cdot\exp(-0.0057\cdot T)$. For choices of values of z_1 between 1,800 and 2,200 m, the fitted temperature profiles were practically the same with a particular choice of vertical advection. The average dispersion of the fitted from the measured temperature among the deepest 23 points ($z \geq 1{,}800$ m) was only 0.12°C if we did not take into account the deepest point, or 0.15°C if we took all points. With assumption *i*, the dashed line in Fig. 1 shows the fitted temperature profile that corresponds to a geothermal flux $q_B = 61$ mW/m^2. Among the four choices (*i–iv*), q_B was the same to within ≈ 1 mW/m^2, and the basal temperature differed from −9°C by no more than 0.7°C.

From our analysis we conclude that South Pole glacial ice is frozen to bedrock and that values of q_B and basal temperature are insensitive to the choice of vertical advection model.

Horizontal Velocity as a Function of Depth

Assuming Glen's flow law (Eq. **2**) with $n = 3$ and $U = 139$ kJ/mol, and taking downhill velocity $u(0) = 9$ m·yr^{-1} at the surface and $u(\mathrm{H}) = 0$ at bedrock, we use the expression $\mathrm{d}u/\mathrm{d}z = -2A\,|\tau_{xz}|^n$ to find the horizontal velocity profile $u(z)$. A is taken to have the same dependence on temperature and climate as found in ref. 9 and used by us in Eq. **2**. The shear stress τ_{xz} increases linearly with z, reaching ≈ 0.038 MPa at the interface with bedrock. The calculated dependence of u on z is shown in Fig. 2. One sees that horizontal velocity for the AMANDA equipment in South Pole ice changes very slowly except in the bottom few hundred meters. For depths 2,000–2,400 m, the fractional increase in cable length is estimated to be only $\approx 0.1\%$ after 20 yr. Copper wire and plastic insulation can easily withstand such strains without breaking. At relevant temperatures of −20° to −30°C we expect that the shear stress at the deepest depths will result in a slight plastic flow of ice around the spherical pressure vessels.

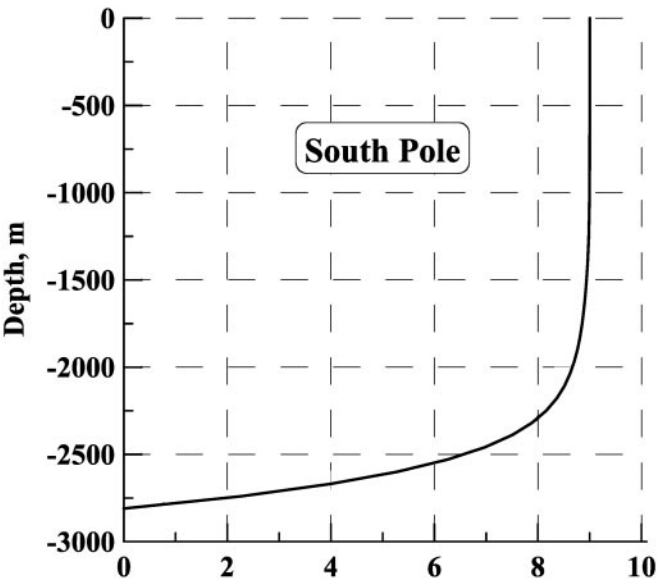

Fig. 2. Horizontal velocity profile calculated from the temperature profile in Fig. 1.

The AMANDA strings end at depths $\approx 2{,}300$ m, and no cables or detectors have failed in the 4 yr since the last strings were installed. When it is built, the 1-km^3 IceCube neutrino observatory will extend to depths of $\approx 2{,}400$ m and should remain intact for longer than 20 yr, even allowing for an estimated uncertainty of as much as a factor 2 in $u(z)$. The main effect of the increase of horizontal flow rate with depth will be that the lowest optical modules will lag increasingly with respect to modules located at shallower depths, where the colder ice is flowing approximately as a rigid body. The AMANDA collaboration plans to monitor changes in relative positions of the modules with time with downgoing muons.

In principle, glacial ice can slide even at subfreezing temperatures. However, from both theory (15, 16) and experiment (17), we estimate that at a temperature of −9°C the thickness of the liquid water layer between ice and bedrock is only ≈ 1 nm and the sliding rate is only a few mm per year, even when impurities are taken into account.

Discussion

A Fossil Lake with a Flat Permafrost Bed as a Habitat for Microbial Life. Of the roughly 100 likely lakes under the Antarctic ice cap detected by airborne radar (18, 19), the largest is Lake Vostok (18), which has generated great interest as a potential and unusual habitat for life. The lake is at least 10^3 m deep at one end, with several hundred meters of glacial sediments over its floor. International planning is underway to search in it for microbial life that may have evolved in isolation from surface life for as long as 20 million yr. It is thought, however, that some or most of the lakes may be hydraulically interconnected. If so, unsterile drilling would contaminate many of them.

We considered whether it is possible to have a subglacial lake of liquid water at the pressure-melting temperature (−2°C) only 10 km from basal ice at −9°C at the South Pole. In principle, the basal ice temperature 10 km away could be higher if the ice was thicker over the lake than at the South Pole, because of the additional insulation. From Fig. 1 we estimate that an additional thickness of 260 m would raise the temperature to the melting point, if the geothermal flux was kept the same. The BEDMAP

data show, however, that the ice is actually 50 m thinner in the region of the lake than at the South Pole.

We next examined whether a higher geothermal heat flux under the lake than at the South Pole could maintain part of the glacial ice at the pressure-melting temperature. Applying the steady-state heat-flow model to bedrock, we found that, although physically not inconceivable, a temperature difference as great as 7°C over a distance of 10 km is highly unlikely to achieve and maintain with a heat source localized in rock under the lake. In the special case of a vertically oriented rocky cylinder of radius 4 km, thickness ≥30 km, and excess radioactive heat output ≈4 $\mu W \cdot m^{-3}$, the lake region could be maintained 7°C warmer than the bedrock under South Pole ice. However, the finely tuned geometry—a warm, vertical pipe in just the right location—is very unlikely.

A sufficiently high concentration of ions soluble in water could, in principle, depress the freezing point by as much as 7°C. The amount required is roughly 2 mol/liter of dissolved ions, which is a factor $\approx 2 \times 10^6$ greater than is observed in typical glacial ice (20). Even in the highly saline ocean, the freezing point is depressed by only ≈2°C.

We are thus led to the conclusion that the flat radar profile is caused by a "fossil lake" that predated permanent Antarctic glaciation some millions of years ago. The strong radar backscatter likely indicates a flat bed of subglacial permafrost—a mixture of granular rock and ice. Its close proximity to the South Pole Station offers the opportunity to develop and test sterile drilling techniques there and to search for exotic microbial life without the risk of contamination of other lakes. Both archaea and bacteria have been found in concentrations up to $\approx 10^8$ cells$\cdot g^{-1}$ at temperatures ≈−10°C in Siberian permafrost (21) and up to 10^5 cells$\cdot g^{-1}$ in Antarctic surface permafrost.[‡‡]

The facilities available at the South Pole and its easy air access from McMurdo Station offer another advantage. Furthermore, the fossil lake is an analog of a permanent Martian polar icecap, within which microbial life may have arisen and may still exist. In contrast, Lake Vostok (18) consists of fresh water up to 1,200 m deep and is relatively inaccessible. It is also a target for environmentalists who are concerned about potential damage to the world's largest subglacial lake.

Ice Cube Neutrino Observatory Can Measure Flow Rate of Cold Ice. Because of the extremely low shear rate of ice at low temperature, the temperature dependence of the parameters A and n in Eq. **2** has not been tested in large volumes of glacial ice well below the freezing point. In a recent landmark experiment, Harper *et al.* (22) used inclinometers in 31 boreholes in a volume of 6×10^6 m^3 of a temperate ($\theta \approx 0$°C) Alaskan glacier to make the first full three-dimensional, high-resolution study of the internal flow field of a glacier. Analyses of trajectories of cosmic ray-produced muons passing through the AMANDA array have been used to map the relative positions of the phototubes, but not yet as a function of time. Being frozen into the ice, each phototube serves as a marker of local flow rate. Numerical simulations indicate that it should be possible to record relative positions of phototubes with a standard deviation as small as 0.2 m. Application of the muon method to the ≈5,000 phototubes in the future IceCube observatory will not only serve the principal need for phototube location for neutrino astronomy but will make it possible for the first time to map the shear rate of ice at temperatures ≈−20° to −30°C throughout a volume of 0.5 km^3, nearly 10^2 times larger than the volume instrumented by Harper *et al.* (22).

We thank members of the AMANDA collaboration for their cooperation. We acknowledge useful discussions with D. Blankenship, K. Cuffey, T. Gow, M. Giovinetto, H. Ueda, L. Hansen, and R. Kelty. Part of this work was supported by National Science Foundation Grant PHY99-71390.

[‡‡] Friedmann, E. I., Gilichinsky, D. A., Wilson, G. S., Ostroumov, V., Vorobyova, E. A., Soina, V. S., Shcherbakova, V. A., Vishnivetskaya, T. A., Chanton, J. P., Friedmann, R. O. *et al.* Eighth International Society for Subsurface Microbiology meeting, Orleans, France, July 7–12, 1996, abstr. 5–1, p. 60.

1. Andrés, E., Askebjer, P., Bai, X., Barouch, G., Barwick, S. W., Bay, R. C., Becker, K.-J., Bergström, L., Bertrand, D., Bierenbaum, D., *et al.* (2001) *Nature (London)* **410,** 441–443.
2. Woschnagg, K., Andrés. E., Askebjer, P., Bai, X., Barouch, G., Barwick, S. W., Bay, R. C., Becker, K.-J., Bergström, L., Bertrand, D., *et al.* (1999) in *Proceedings of the 26th International Cosmic Ray Conference*, *Salt Lake City*, eds. Kieda, D., Salamon, M. & Dingus, B. (University of Utah, Salt Lake City), Vol. 2, pp. 200–203.
3. Price, P. B., Woschnagg, K. & Chirkin, D. (2000) *Geophys. Res. Lett.* **27,** 2129–2132.
4. Giovinetto, M. (1960) *Report 825–2-Part IV, IGY Project No. 4.10, U.S. National Committee for the International Geophysical Year* (*USNC-IGY) Antarctic Glaciological Data, Field Work (1958)* and *1959 (South Pole Station)* (Ohio State Univ. Research Foundation, Columbus).
5. Budd, W. F. & Young, N. W. (1983) in *The Climatic Record in Polar Ice Sheets*, ed. Robin, G. deQ. (Cambridge Univ. Press, Cambridge, U.K.), pp. 150–177.
6. Nagornov, O. V., Konovalov, Yu. V., Zagorodnov, V. S. & Thompson, L. G. (2001) *J. Eng. Phys. Thermophys.* **74,** 253–265.
7. Hansen, B. L. & Langway, C. C., Jr. (1996) *Antarctic J.* **1,** 207–208.
8. Lythe, M. B., Vaughan, D. G. & BEDMAP Consortium (2001) *J. Geophys. Res.* **106,** 11335–11351.
9. Paterson, W. S. B. (1994) *The Physics of Glaciers* (Pergamon, Oxford), 3rd Ed.
10. Hanson, B. & Dickinson, R. E. (1987) *J. Glaciol.* **33,** 140–148.
11. Dansgaard, W. & Johnsen, S. J. (1969) *J. Glaciol.* **8,** 215–223.
12. Mosley-Thompson, E., Paskievitch, J. F., Gow, A. J. & Thompson, L. G. (1999) *J. Geophys. Res.* **104,** 3877–3886.
13. Raisbeck, G. M., Yiou, F., Bourles, D., Lorius, C., Jouzel, J. & Barkov, N. I., (1987) *Nature (London)* **326,** 273–277.
14. Kuivinen, K. C., Koci, B. R., Holdsworth, G. W. & Gow, A. J. (2001) *Antarctic J. (United States)* **17,** 89–91.
15. Shreve, R. L. (1984) *J. Glaciol.* **30,** 341–347.
16. Wettlaufer, J. S. (1999) *Phys. Rev. Lett.* **82,** 2516–2519.
17. Cuffey, K., Conway, H., Hallet, B., Gades, A. M. & Raymond, C. F. (1999) *Geophys. Res. Lett.* **26,** 751–754.
18. Kapitsa, A. P., Ridley, J. K., Robin, G. Q., Siegert, M. J. & Zotikov, I. A. (1996) *Nature (London)* **381,** 684–686.
19. Siegert, M. J. (2000) *Earth Sci. Rev.* **50,** 29–50.
20. Price, P. B. (2000) *Proc. Natl. Acad. Sci. USA* **97,** 1247–1251.
21. Zvyagintsev, D. G., Gilichinsky, D. A., Khlebnikova, G. M., Fedorov-Davydov, D. G. & Kurdryavtseva, N. N. (1990) *Microbiology* **59,** 332–338.
22. Harper, J. T., Humphrey, N. F., Pfeffer, W. T., Huzurbazar, S. V., Bahr, D. B. & Welch, B. C. (2001) *J. Geophys. Res.* **106,** 8647–8562.